Phase Equilibria of Dilute Poly(ethylene-*co*-1-butene) Solutions in Ethylene, 1-Butene, and 1-Butene + Ethylene

Ai-Qi Chen and Maciej Radosz*

Department of Chemical Engineering, Louisiana State University, Baton Rouge, Louisiana 70803-7303

Fluid−liquid and solid−fluid transitions were measured for dilute poly(ethylene-*co*-1-butene) solutions in ethylene, 1-butene, and ethylene + 1-butene from about −50 °C to about 180 °C and up to 1500 bar. The experimental fluid−liquid data were correlated with a copolymer SAFT equation of state.

Introduction

Polyolefins are miscible in all proportions with ethylene and ethylene + comonomer mixtures but only at pressures and temperatures that are sufficiently high. The minimum pressures and temperatures for a state of complete miscibility (one-phase state) can be estimated from phase-boundary curves that correspond to phase transitions. Such phase transitions are usually measured as the onset of phase separation, in going from a one-phase region (clear, homogeneous solution) to a two-phase region (turbid, "cloudy" solution, hence the term "cloud-point"). Different forms of the polyolefin phase transitions at high pressures, for example, fluid−liquid transitions of the lower-critical-solution-temperature (LCST) type and of the upper-critical-solution-temperature (UCST) type and solid−fluid transitions, and different phase diagrams for polyolefin solutions are discussed by Folie and Radosz (1995).

One of the problems in the high-pressure polyethylene processes is polymer deposition on the heat exchanger walls, referred to as fouling. For example, the heat-exchanger fouling in the recycle section is caused by polymer precipitation from the dilute recycle solution that is generated as a high-pressure separator overhead stream. Such recycle streams usually contain a low (less or much less than 1 wt %) but variable content of the polymer light end, referred to as wax. Moreover, such recycle streams also vary widely in polymer crystallizability (usually lower than that of the bulk product) and in solvent composition. All these variables have a strong effect on the extent of fouling. To mitigate such fouling, it is necessary to understand the phase transitions that the recycle stream undergoes on its heat-exchanger path, from the high-pressure separator to the compressor.

Since there have been no published data for such dilute systems, one objective of this work is to measure the fluid−liquid and solid−fluid pressures and temperatures for a large number of dilute solutions varying in polymer concentration, solvent type, and polymer crystallizability. The polymer concentration is from as low as 0.01 (usually 0.1) to about 1 wt %. The solvents selected for this work are ethylene and 1-butene and a mixture of ethylene + 1-butene. The polymer samples are of the poly(ethylene-*co*-1-butene) type with a number of ethyl branches from about 4 (high crystallizability) to about 78 (no crystallizability). Other objectives of this work are to correlate the fluid−liquid (but not solid−fluid) experimental data with a copolymer equation of state that captures all the effects probed experimentally and to test if the ternary data can be predicted.

* Corresponding author. E-mail: radosz@che.lsu.edu.

Experimental Section

Apparatus and Method. Phase boundaries were measured in a batch optical cell equipped with a sapphire window, which makes it possible to observe phase transitions visually, and with a movable piston, which makes it possible to adjust pressure at constant composition by varying the system volume. A more detailed description of the equipment used in this work is given by Gregg et al. (1994a), who also characterize the temperature accuracy to be less than 0.1 K and the pressure accuracy to be less than 1 bar.

In operation, known amounts of polymer and solvent are loaded into the cell and stirred with a magnetic stir bar. The temperature is set equal to a desired target, and the pressure is increased by moving the piston toward the window to such an extent that all the components are completely miscible and form a homogeneous solution. Once the solution is equilibrated at an arbitrary but sufficiently high pressure, the pressure is slowly reduced at constant temperature by allowing the piston to move away from the window and hence by slowly decreasing the system volume and decreasing its density, while continuing stirring. Upon crossing the cloud-point phase boundary, the solution turns turbid, which is observed visually through an optical device called a borescope. The pressure corresponding to this transition is recorded as the cloud-point pressure. Next, the experiment is repeated on the same sample at another temperature level.

If the fluid−liquid interface moves downward with a further drop in pressure, we refer to such a transition as being of a bubble-point type; the solvent-rich phase is the minor phase at the onset of phase separation. Conversely, if the interface moves upward with a further drop in pressure, we refer to such a transition as being of a dew-point type; the polymer-rich phase is the minor phase at the onset of phase separation. Since this work is mostly limited to dilute solutions, for which the highest weight percent of solute is not much higher than 1, the phase transitions observed in this work are usually of the dew-point type.

The solid−fluid phase transitions are measured differently than the fluid−liquid transitions. The piston is approximately fixed, but the temperature is slowly decreased (say, around 1 K·min^{-1}), so the cooling rate effect

10.1021/je9803126 CCC: $18.00
Published on Web 06/03/1999

Table 1. Polymer Properties[a]

polymer	M_n	MWD	BD	DP	mol % 1,2 units	T_m or T_c peak/°C	T_g peak/°C
C40	563.1	1.00	0	20		81−83	
PIB	1000	1.12	100	24		amorphous	
EB04	6430	1.04	4.5	220	8.6	$T_m = 103$	
						$T_c = 96$	
EB17	7570	1.04	17.0	231	29.0	$T_m = 45$	
						$T_c = 30$	$\gamma - T_g = -43$
EB78	11500	1.04	77.8	231	87.5	amorphous	$\beta - T_g = 39$

[a] M_n is the number average molecular weight; MWD is the molecular weight distribution; BD is the branch density, equal to the number of branches per 100 ethyl units in the backbone; DP is the degree of polymerization, defined as the total number of ethyl units in the backbone; mol % 1,2 units is the mole percent of 1,2 addition in polybutadiene; T_c, T_g, and T_m are the crystallization, glass transition, and melting temperatures; EB04 has about 7.2% (by weight) impurities detected by DSC (probably polymer with lower molecular weight).

is negligible, starting from a one-phase region. As a result, the pressure decreases slightly too. The onset of solid formation corresponds to the crystallization temperature. Next, the experiment is repeated at another pressure level. A similar approach is used for steep, low-temperature phase boundaries in solutions of amorphous polymers, for example, the upper-critical-solution-temperature (UCST) boundaries. In this work, we are not interested in the solid−fluid transitions upon heating, which usually take place at somewhat higher temperatures, because they are less relevant to fouling.

Materials. The solvents used in this work are either ethylene (polymer grade from Matheson with a known minimum purity of 99.9%) or 1-butene (also from Matheson with a known minimum purity of 99%) or a mixture of both. The C_{40} sample is tetracontane from Aldrich.

Most polymer samples used in this work are primarily poly(ethylene-*co*-1-butene) with variable 1-butene content and, hence, variable branch density (BD). We define the branch density as the number of ethyl branches per one hundred ethyl units in the backbone (in this case, same as the number of carbons in the branches per number of carbons in the backbone). These samples were prepared by hydrogenating polybutadiene obtained from anionic synthesis by Polymer Source, Inc., 771 Lajoie, Dorval, Quebec, Canada H9P 1G7. Their properties are given in Table 1, where the label gives the polymer type (for example, EB) and an approximate branch density (for example, EB04). The branch density varies from 4.5 on the low side, which corresponds to a high degree of crystallizability, through a BD of 17, which corresponds to a low degree of crystallizability, to BD of 77.8 on the high side, which corresponds to an amorphous polymer. All these EB samples are nearly monodisperse, with a molecular weight distribution (MWD) of 1.1 or less, and have about 220−230 ethyl units in the backbone. Since the backbone length is approximately constant, their number average molecular weight (M_n) increases with increasing BD.

The branch density is calculated on the basis of the mole percent of 1,2 addition (A_{12}) as follows:

$$\mathrm{BD} = \frac{100A_{12}}{200 - A_{12}}$$

For the record, the molecular weight and MWD of the EB samples were determined prior to hydrogenation in gel permeation chromatography columns calibrated with monodisperse polybutadiene standards and then were corrected for added hydrogen. Further analysis by Fourier transform infrared spectroscopy confirmed complete hydrogenation. Proton nuclear magnetic resonance spectroscopy was used to determine the mole percent of 1,2 addition in polybutadiene, prior to hydrogenation. This mole percent of 1,2 addition is estimated to be accurate to within ±2. Finally, the melting, crystallization, and glass transitions were derived from DSC. All these data are reported in Table 1. Also included in Table 1 is a pair of smaller molecules (about 20−24 ethyl units in the backbone), of which one is a straight chain alkane (normal C_{40}) and one is an amorphous branchy alkane of the polyisobutylene (PIB) type. The PIB sample is the same as the blank PIB described by Gregg et al. (1994b).

Table 2. SAFT Pure-Component Parameters[a]

compound	branch density	x_E	x_B	M	$v°$	$(u^0/k)_E$	$(u^0/k)_B$
ethylene	0			1.464	18.16	212.1	
1-butene	0			3.162	13.15	202.5	
C40	0			26.97	12.00	220.0	
PIB	100			49.35	12.00	225.0	
EB04	4.5	0.9570	0.0430	300.6	12.00	215.0	160.0
EB17	17.0	0.8550	0.1450	353.8	12.00	215.0	160.0
EB78	77.8	0.5624	0.4376	537.1	12.00	215.0	160.0

[a] The effective segment numbers (m) and segment volumes ($v°$) for all chemicals are obtained by Huang and Radosz (1990, 1991); the dispersion energy parameters of segments (u^0/k) are obtained by Huang and Radosz (1990, 1991) for ethylene and 1-butene, by Gregg et al. (1994b) for PIB, and by correlating the experimental results in this work for C40, EB04, EB17, and EB78.

SAFT Modeling

The experimental data taken in this work were correlated with an equation of state developed on the basis of the statistical associating fluid theory (SAFT). The specific version of the SAFT equation of state used in this work is that described by Banaszak et al. (1996) and referred to as the copolymer SAFT.

The copolymer SAFT requires three pure-component parameters, the segment energy u/k, the segment volume v°, and the segment number m. The segment energy in the backbone $(u/k)_E$, however, has a different value than the segment energy in the branch $(u/k)_B$. The copolymer SAFT also requires the number fraction of the backbone segments (x_E) and the number fraction of the branch segments (x_B) for each polymer. For EB copolymers, they are calculated as follows with $x_B = \mathrm{BD}/(100 + \mathrm{BD})$ and $x_E = 1 - x_B$.

The pure-component SAFT parameters are given in Table 2. There are also binary interaction parameters k_{ij} that are estimated or fitted to the experimental data. We note that the binary parameters for the branch and backbone segments, for example, $k_{E-\mathrm{solvent}}$ and $k_{B-\mathrm{solvent}}$, may or may not be equal.

Results

All the experimental results are tabulated in the Supporting Information. The phase behavior effects and calculated results are discussed below.

Amorphous PIB is found to exhibit a simple LCST behavior with ethylene**.** This is shown in Figure 1 where

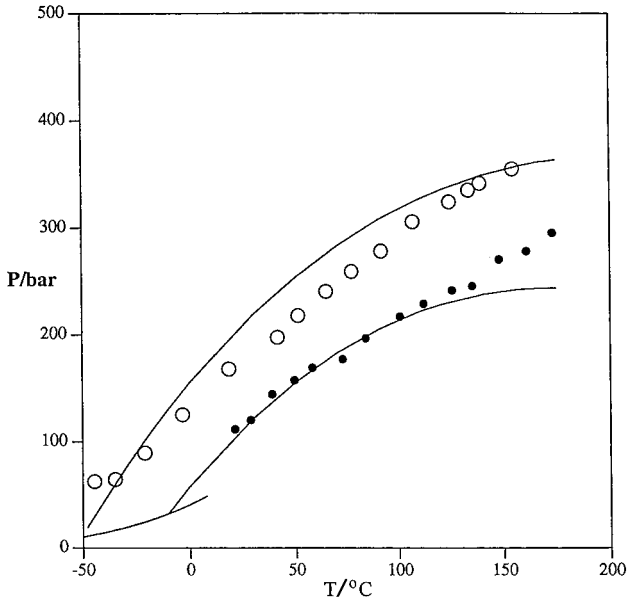

Figure 1. Phase-transition pressure of polyisobutylene in ethylene: concentration effect. Open circles, 0.25 wt %; filled circles, 0.0013 wt %; solid curves, reference vapor pressure curve for ethylene and cloud-point curves (the latter calculated from the SAFT correlation with $k_{ij} = 0.0133$).

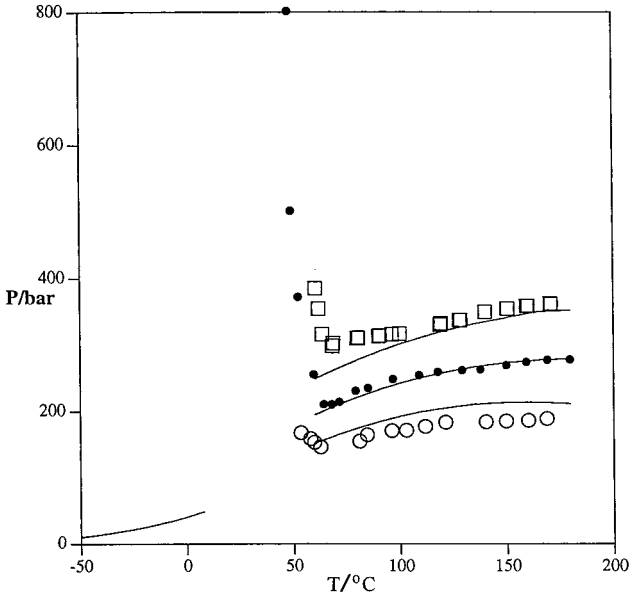

Figure 2. Phase-transition pressure of normal-$C_{40}H_{82}$ (C40) in ethylene: concentration effect. Open circles, 0.15 wt %; filled circles, 1.1 wt %; squares, 5.6 wt %; solid curves, reference vapor pressure curve for ethylene and cloud-point curves (the latter calculated from the SAFT correlation with $k_{ij} = 0.002$).

the cloud-point phase boundaries are plotted in pressure and temperature coordinates for two PIB concentrations, 0.25% and 0.0013%. From this point on, the symbol % will mean weight percent. The experimental points exhibit a little scatter because this was our first series of experiments at such low concentrations and the visual cloud-point detection was somewhat uncertain; we refined our approach in other experiments but chose to include these data as well. The solid curves are calculated with the original SAFT equation of state, that is, the homopolymer SAFT, proposed by Huang and Radosz (1990, 1991) and also used by Gregg et al. (1994b). We have not attempted to model PIB as a branched molecule but rather as an effective

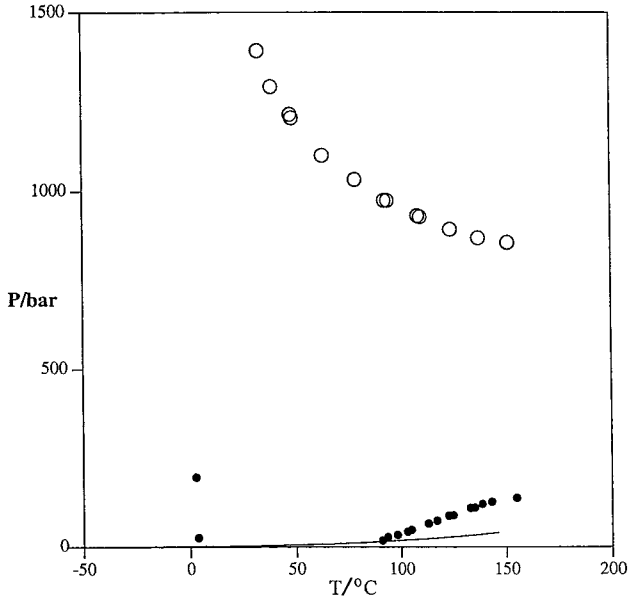

Figure 3. Phase-transition pressure of EB17 in ethylene (open circles, 0.79 wt %) and in 1-butene (filled circles, 0.78 wt %). Only the vapor pressure curve for 1-butene is shown.

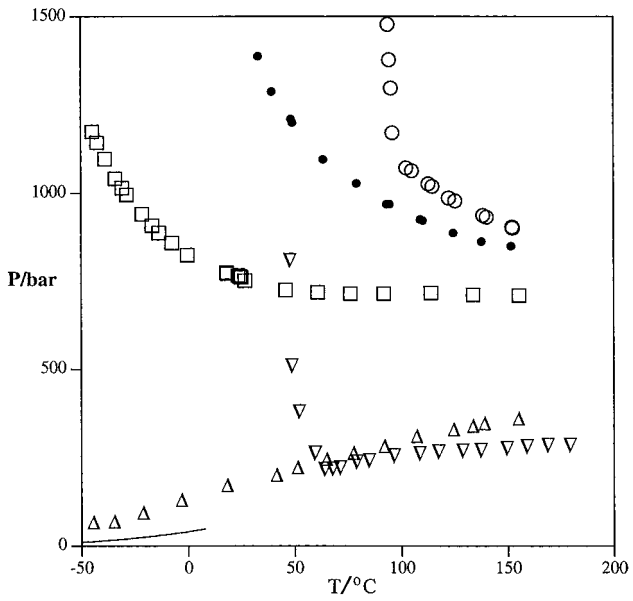

Figure 4. Phase-transition pressure in ethylene: branch density effect for EB04 (open circles, 0.65 wt %), EB17 (filled circles, 0.79 wt %), EB78 (squares, 0.91 wt %), C40 (triangles pointing down), and PIB (triangles pointing up).

homopolymer. We note that decreasing PIB % decreases the cloud-point pressure, which means that, as expected, these transitions are of the dew-point type, that is, below the critical polymer concentration. An increasing curve at the bottom left corner of this and other figures is the reference vapor pressure curve for the solvent.

Crystalline alkane C40 is also found to exhibit LCST behavior with ethylene but at high temperatures only. At lower temperatures, however, this system exhibits a typical solid−fluid transition, with a negative steep slope, in the 50−65 °C range. This is shown in Figure 2. The points are the experimentally determined phase transitions, and the curves are calculated from SAFT. The higher concentration solution (about 5%) has cloud-point pressures similar to those reported by de Loos et al. (1983). The solid−fluid transitions were measured by decreasing temperature

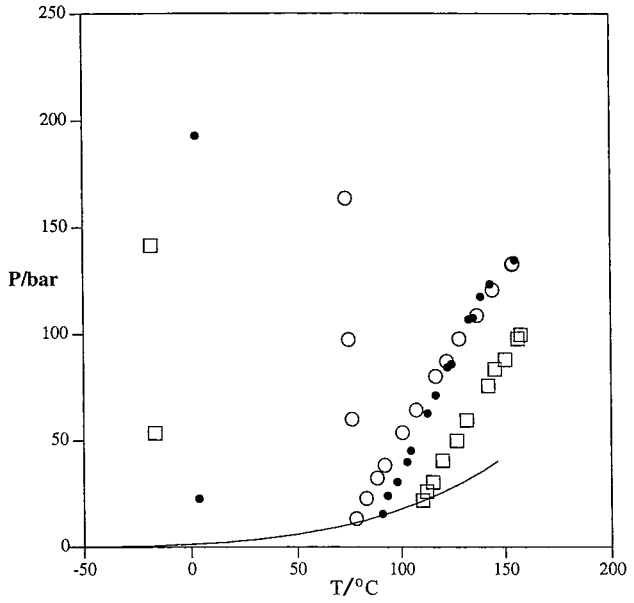

Figure 5. Phase-transition pressure in 1-butene: branch density effect for EB04 (open circles, 1.05 wt %), EB17 (filled circles, 0.78 wt %), and EB78 (squares, 1.32 wt %).

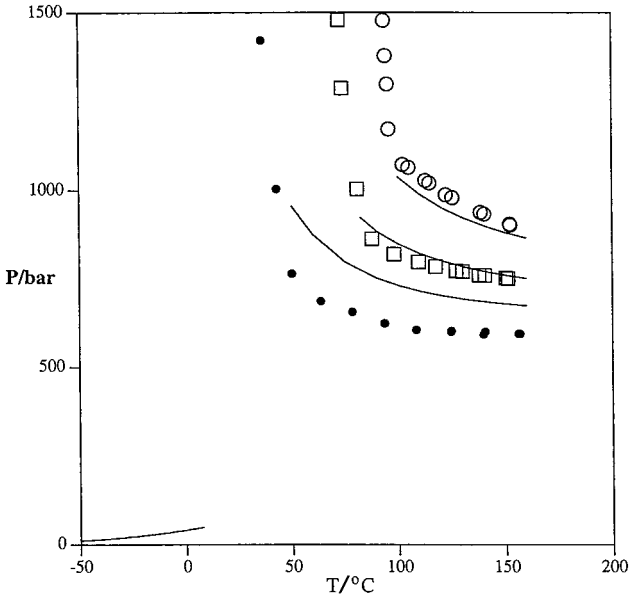

Figure 6. Phase-transition pressure of EB04 in ethylene: concentration effect; open circles, 0.65 wt %; squares, 0.096 wt %; filled circles, 0.015 wt %; solid curves, reference vapor pressure curve for ethylene and cloud-point curves (the latter calculated from the SAFT correlation with $k_{ij} = 0.061$).

while the fluid−liquid transitions were measured by decreasing pressure; these transitions are not included for the lowest concentration because they were difficult to detect. These solid−fluid transitions are not calculated in this work.

As expected, 1-butene solutions are found to have much lower cloud-point pressures than the ethylene solutions. An example is shown in Figure 3 for 1% solutions of EB17. The 1-butene solutions exhibit both LCST and solid−fluid boundaries but are found to be completely miscible above the vapor pressure of 1-butene over a broad temperature range of at least 5−90 °C. Even above about 90 °C, only moderate pressures are required for complete miscibility. By contrast, the ethylene solution of EB17 exhibits a UCST behavior (above the solid−fluid temperatures), and it is

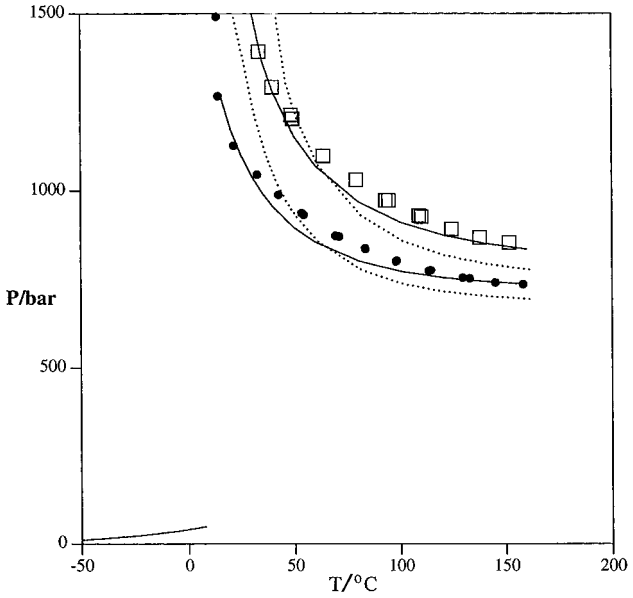

Figure 7. Phase-transition pressure of EB17 in ethylene: concentration effect. Filled circles (two separate experiments), 0.13 wt %; squares, 0.79 wt %; solid curves, reference vapor pressure curve for ethylene and cloud-point curves calculated from the SAFT correlation with a temperature-dependent $k_{ij} = 0.059 + (6 \times 10^{-5})(t - 35)$, where t is in °C; dotted curves, cloud-point curves calculated from the SAFT correlation with a constant, temperature-independent $k_{ij} = 0.061$ (same as in Figure 6).

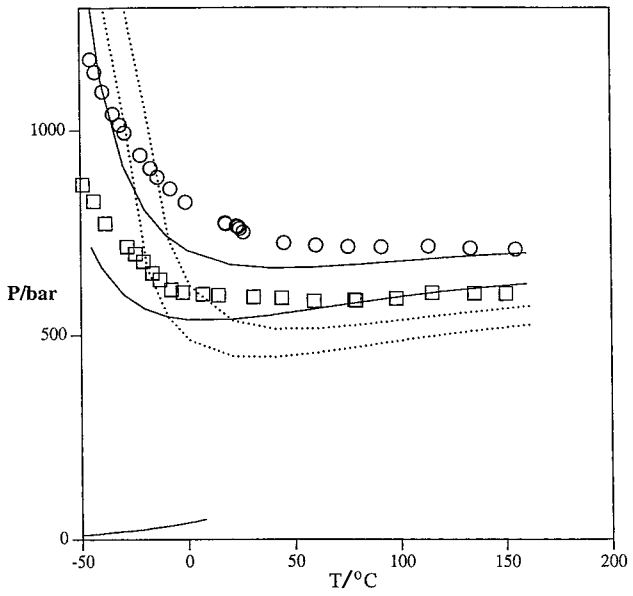

Figure 8. Phase-transition pressure of EB78 in ethylene: concentration effect. Open circles, 0.91 wt %; squares, 0.12 wt %; solid curves, reference vapor pressure curve for ethylene and cloud-point curves calculated from the SAFT correlation with $kij = 0.056 + 0.0001463(t + 45)$, where t is in °C; dotted curves, cloud-point curves calculated from the SAFT correlation with $k_{ij} = 0.061$ (same as in Figure 6).

immiscible below the cloud-point pressure, which is higher than 700 bar in the temperature range investigated in this work. In other words, 1-butene is a much better solvent than ethylene for EB17.

Increasing branch density (BD) is found to drastically reduce the cloud-point pressure in ethylene solutions, especially at lower temperatures. This is shown in Figure 4 for the three EB polymers, at around 1% each. For example, around 100 °C, the EB04 cloud-point pressure

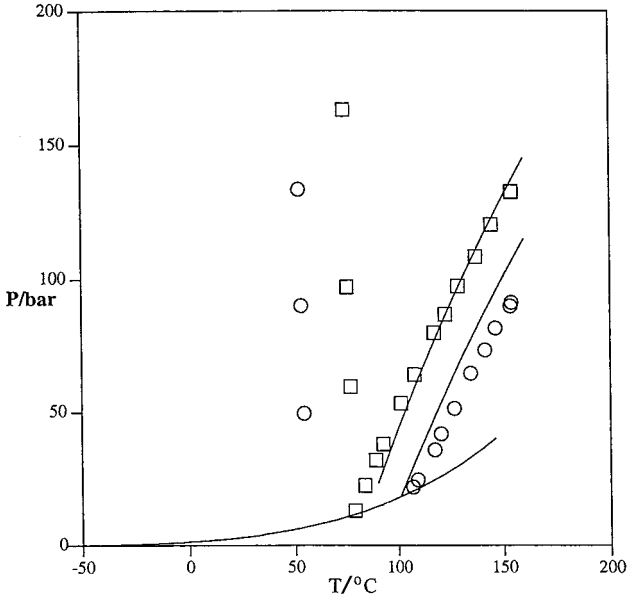

Figure 9. Phase-transition pressure of EB04 in 1-butene: concentration effect. Open circles, 0.075 wt %; squares, 1.05 wt %; solid curves, reference vapor pressure curve for 1-butene and cloud-point curves calculated from the SAFT correlation with $k_{ij} = 0$.

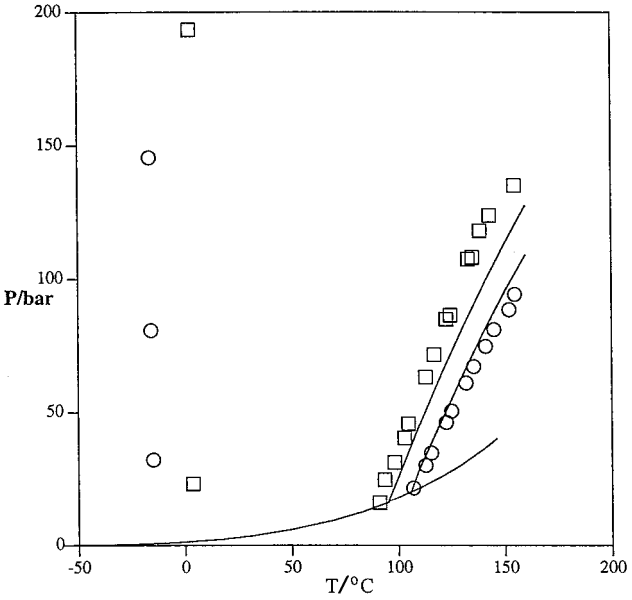

Figure 10. Phase-transition pressure of EB17 in 1-butene: concentration effect. Open circles, 0.11 wt %; squares, 0.78 wt %; solid curves, reference vapor pressure curve for 1-butene and cloud-point curves calculated from the SAFT correlation with $k_{ij} = 0$.

(open circles) is above 1000 bar while the EB78 cloud-point pressure (squares) is around 700 bar. The steep SL curve is observed around 95−97 °C for EB04. The SL curve for EB17 has not been measured but is expected to be present around the crystallization range for EB17, that is, around 30 °C at pressures above 1500 bar. In any event, we do not observe a significant lowering of the pure-polymer crystallization temperature in the presence of ethylene in this concentration range. The cloud point curve for EB78 is quite flat at higher temperatures. It starts increasing upon lowering temperature around the pure-EB78 $\beta-T_g$ transition, and it reaches an even steeper negative slope around the pure-EB78 $\gamma-T_g$ transition.

By way of reference, the two curves at the bottom of Figure 4 are to illustrate the extent to which the cloud-

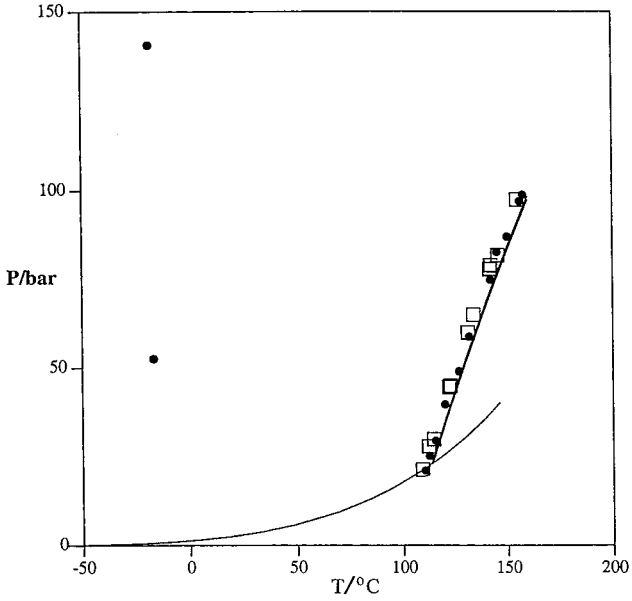

Figure 11. Phase-transition pressure of EB78 in 1-butene: concentration effect. Squares, 1.3 wt %; filled circles, 1.1 wt %; solid curves, reference vapor pressure curve for 1-butene and cloud-point curves calculated from the SAFT correlation with $k_{ij} = 0$. Experimental data at around 0.07 wt %, found nearly to coincide with those at around 1 wt % shown in this figure, are not included because they are probably less reliable.

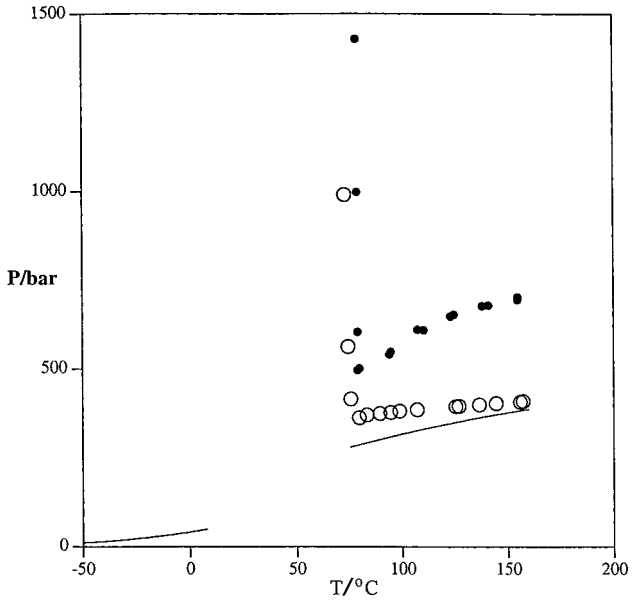

Figure 12. Phase-transition pressure of EB17 in mixtures of ethylene + 1-butene: concentration effect. Open circles, 0.085 wt % EB17, 49/51 weight/weight ethylene/1-butene ratio; filled circles, 0.927 wt % EB17, 40/59 weight/weight ethylene/1-butene ratio; solid curves, reference vapor pressure curve for ethylene and a cloud-point curve calculated from the SAFT correlation for the open-circle case with $k_{\mathrm{EB-ethylene}} = 0.059 + (6 \times 10^{-5})(t - 35)$, where t is in °C, $k_{\mathrm{EB-1-butene}} = 0$, and $k_{\mathrm{ethylene-1-butene}} = 0.03$. The SAFT curve for the filled-circle case is close to that shown in this figure.

point pressure decreases upon decreasing the backbone length, in this case, by a factor of 10 or so. The C40 (triangles pointing down) and PIB (triangles pointing up) curves nearly coincide above the SL transition for C40. We note that the PIB concentration is only about 0.25% in this case; a 1% curve is expected to be shifted toward higher pressures. Nevertheless, the point is that, as we decrease the backbone length approximately by an order of magni-

tude in this molecular weight range (from about 200 to about 20), the cloud-point pressure decreases roughly by a factor of 2 (from about 700−1000 to about 250−400 bar).

Increasing BD slightly reduces the LCST-type cloud-point pressure in 1% 1-butene solutions. We observe it as a shift, from circles to squares in Figure 5, of the increasing curves at temperatures above 70 °C. Increasing BD has a much stronger effect on the low-temperature transitions, solid−liquid for EB04 and EB17, and UCST for EB78. Furthermore, 1-butene seem to depress the pure-EB crystallization temperature by about 20 °C; that is, the solid−liquid transition upon lowering the temperature of the 1-butene solutions is about 20 °C lower than the crystallization peak observed with DSC.

Increasing polymer concentration systematically increases the cloud-point pressure and shifts the SL and UCST transitions to lower temperatures. This is expected for all the transitions at polymer concentrations below that corresponding to a maximum on a PX isotherm. The polymer concentrations investigated in this work, up to about 1%, should be below that corresponding to a maximum on a PX isotherm. This finding is illustrated for ethylene + EB04 in Figure 6, for ethylene + EB17 in Figure 7, and for ethylene + EB78 in Figure 8. A similar trend is observed for 1-butene, as is shown in Figures 9−11, except the shift due to a change in polymer concentration is lower because the phase transition pressures are much lower, especially for EB17.

SAFT correlation captures the BD effects for both solvents. This is shown in Figures 6−11. The accuracy depends on the extent to which k_{ij} is allowed to vary with temperature. For example, the ethylene + EB04 curves are correlated with a constant k_{ij}. The same constant k_{ij} qualitatively represents the ethylene + EB17 and ethylene + EB78 curves as well, but a more accurate representation can be obtained with a temperature-dependent k_{ij}. This is shown in Figures 7 and 8. SAFT is even more predictive for the 1-butene systems. In fact, k_{ij} set equal to zero allows for essentially quantitative predictions, as is shown in Figures 9−11. In all the SAFT calculations presented here, we only model the fluid−liquid transitions. The solid−liquid transitions are being included in the next version of the SAFT model.

SAFT also predicts the ternary cloud-point pressure. This is shown for a 0.085% solution of EB17 in a mixture of ethylene + 1-butene (about 50/50 by weight) in Figure 12 with open circles. The k_{ij} values used for this prediction are the same as those for the 1-butene and ethylene binaries (the temperature-dependent k_{ij} for ethylene) without further readjustment. The experimental data shown as filled circles in Figure 12, for 0.927% EB17, are for a somewhat lower ethylene/1-butene ratio (about 40/59 by weight). The SAFT prediction in this case, assuming such a low ethylene/1-butene ratio, suggests a cloud-point curve that nearly coincides with that for the former case, well below the experimental points (filled circles) and close to the open circles (hence, not shown in Figure 12). This inconsistency can probably be explained by a small inaccuracy in feeding that caused the ethylene weight percent to be underestimated in calculating the experimental mixture composition. For the record, the value of k_{ij} for the ethylene + 1-butene binary used in all the ternary predictions, equal to 0.03, is obtained by fitting the experimental ethylene + 1-butene data of Laugier et al. (1994).

Conclusions

The effects of polymer concentration, branch density, hence crystallizability, and solvent type on the phase-transition pressures have been quantified experimentally for a series of poly(ethylene-*co*-1-butene) samples. As expected, the 1-butene solutions require much lower pressures than the ethylene solutions for complete miscibility. Also, increasing branch density (decreasing crystallizability) reduces the phase-transition pressures. The copolymer SAFT model is found to correlate the experimental data.

Acknowledgment

The authors are grateful to Ioan Negulescu for the DSC characterization of the EB polymers used in this work and to Bernard Folie for his comments.

Supporting Information Available:

Tabulated experimental data are available free of charge at http://pubs.acs.org.

Literature Cited

Banaszak, M.; Chen, C. K.; Radosz, M. Copolymer SAFT Equation of State. Thermodynamic Perturbation Theory Extended to Heterobonded Chains. *Macromolecules* **1996**, *29*, 6481−6486.

de Loos, T. W.; Poot, W.; Diepen, A. M. Fluid Phase Equilibria in the System Polyethylene + Ethylene. 1. Systems of Linear Polyethylene + Ethylene at High Pressures. *Macromolecules* **1983**, *16*, 111−117.

Folie, B.; Radosz, M. Phase Equilibria in High-Pressure Polyethylene Technology. *Ind. Eng. Chem. Res.* **1995**, *34*, 1501−1516.

Gregg, C. J.; Stein, F. P.; Morgan, C. K.; Radosz, M. A Variable Volume Optical PVT Cell for High-Pressure Cloud Point, Densities, and Infrared Spectra; Applicable to Supercritical Fluid Solutions of Polymers up to 2 kbar. *J. Chem. Eng. Data* **1994a**, *39*, 219−224.

Gregg, C. J.; Stein, F. P.; Radosz, M. Phase Behavior of Telechelic Polyisobutylene (PIB) in Subcritical and Supercritical Fluids. 1. Inter- and Intra-Association Effects for Blank, Monohydroxy, and Dihydroxy PIB(1k) in Ethane, Propane, Dimethyl Ether, Carbon Dioxide, and Chlorodifluoromethane. *Macromolecules* **1994b**, *27*, 4972−4980.

Huang, S. H.; Radosz, M. Equation of State for Small, Large, Polydisperse, and Associating Molecules. *Ind. Eng. Chem. Res.* **1990**, *29*, 2284−2294.

Huang, S. H.; Radosz, M. Equation of State for Small, Large, Polydisperse, and Associating Molecules: Extension to Fluid Mixtures. *Ind. Eng. Chem. Res.* **1991**, *30*, 1994−2005.

Laugier, S.; Richon, D.; Renon, H. Ethylene + Olefin Binary Systems: Vapor−Liquid Equilibrium Experimental Data and Modeling. *J. Chem. Eng. Data* **1994,** *39*, 388−391.

Received for review December 17, 1998. Accepted April 23, 1999.

JE9803126